



# Electrically tunable binary phase Fresnel lens based on a dielectric elastomer actuator

SUNTAK PARK,<sup>1</sup> BONGJE PARK,<sup>1</sup> SAEKWANG NAM,<sup>1</sup> SUNGRYUL YUN,<sup>1</sup>  
SEUNG KOO PARK,<sup>1</sup> SEONGCHEOL MUN,<sup>1</sup> JEONG MOOK LIM,<sup>1</sup> YEONGHWA  
RYU,<sup>2</sup> SEOK HO SONG,<sup>2</sup> AND KI-UK KYUNG<sup>1,\*</sup>

<sup>1</sup>Electronics and Telecommunications Research Institute (ETRI), 218 Gajeongro, Yuseong-gu, Daejeon 34129, South Korea

<sup>2</sup>Department of Physics, Hanyang University, Seoul 133-791, South Korea

\*kyungku@etri.re.kr

**Abstract:** We propose and demonstrate an all-solid-state tunable binary phase Fresnel lens with electrically controllable focal length. The lens is composed of a binary phase Fresnel zone plate, a circular acrylic frame, and a dielectric elastomer (DE) actuator which is made of a thin DE layer and two compliant electrodes using silver nanowires. Under electric potential, the actuator produces in-plane deformation in a radial direction that can compress the Fresnel zones. The electrically-induced deformation compresses the Fresnel zones to be contracted as high as 9.1% and changes the focal length, getting shorter from 20.0 cm to 14.5 cm. The measured change in the focal length of the fabricated lens is consistent with the result estimated from numerical simulation.

© 2017 Optical Society of America

**OCIS codes:** (050.1965) Diffractive lenses; (230.3990) Micro-optical devices.

## References and links

1. H. Zappe, *Fundamentals of Micro-optics* (Cambridge University Press, 2010).
2. B. Gzybowski, D. Qin, R. Haag, and G. M. Whitesides, "Elastomeric optical elements with deformable surface topographies: applications to force measurements, tunable light transmission and light focusing," *Sens. Actuators A Phys.* **86**(1-2), 81–85 (2000).
3. M. Hain, R. Glockner, S. Bhattacharya, D. Dias, S. Stankovic, and T. Tschudi, "Fast switching liquid crystal lenses for a dual focus digital versatile disc pickup," *Opt. Commun.* **188**(5-6), 291–299 (2001).
4. K. Philipp, A. Smolarski, N. Koukourakis, A. Fischer, M. Stürmer, U. Wallrabe, and J. W. Czarske, "Volumetric HiLo microscopy employing an electrically tunable lens," *Opt. Express* **24**(13), 15029–15041 (2016).
5. S. Yun, S. Park, B. Park, S. Nam, S. K. Park, and K. Kyung, "A thin film active-lens with translational control for dynamically programmable optical zoom," *Appl. Phys. Lett.* **107**(8), 081907 (2015).
6. P. Valley, M. Reza Dodge, J. Schwiegerling, G. Peyman, and N. Peyghambarian, "Nonmechanical bifocal zoom telescope," *Opt. Lett.* **35**(15), 2582–2584 (2010).
7. N. Chronis, G. Liu, K. H. Jeong, and L. Lee, "Tunable liquid-filled microlens array integrated with microfluidic network," *Opt. Express* **11**(19), 2370–2378 (2003).
8. K. Mishra, C. Murade, B. Carreel, I. Roghair, J. M. Oh, G. Manukyan, D. van den Ende, and F. Mugele, "Optofluidic lens with tunable focal length and asphericity," *Sci. Rep.* **4**(1), 6378 (2015).
9. C. A. Lopez, C. Lee, and A. H. Hirs, "Electrochemically activated adaptive liquid lens," *Appl. Phys. Lett.* **87**(13), 134102 (2005).
10. C. Li and H. Jiang, "Electrowetting-driven variable-focus microlens on flexible surfaces," *Appl. Phys. Lett.* **100**(23), 231105 (2012).
11. P. Valley, D. L. Mathine, M. R. Dodge, J. Schwiegerling, G. Peyman, and N. Peyghambarian, "Tunable-focus flat liquid-crystal diffractive lens," *Opt. Lett.* **35**(3), 336–338 (2010).
12. X. Li, L. Wei, R. H. Poelma, S. Vollebregt, J. Wei, H. P. Urbach, P. M. Sarro, and G. Q. Zhang, "Stretchable binary Fresnel lens for focus tuning," *Sci. Rep.* **6**(1), 25348 (2016).
13. K. Rastani, A. Marrakchi, S. F. Habiby, W. M. Hubbard, H. Gilchrist, and R. E. Nahory, "Binary phase Fresnel lenses for generation of two-dimensional beam arrays," *Appl. Opt.* **30**(11), 1347–1354 (1991).
14. B. Li, H. Chen, J. Qiang, S. Hu, Z. Zhu, and Y. Wang, "Effect of mechanical pre-stretch on the stabilization of dielectric elastomer actuation," *J. Phys. D Appl. Phys.* **44**(15), 155301 (2011).
15. K. Jung, J. C. Koo, J.-D. Nam, Y. K. Lee, and H. R. Choi, "Artificial annelid robot driven by soft actuators," *Bioinspir. Biomim.* **2**(2), S42–S49 (2007).
16. S. Rosset, M. Niklaus, P. Dubois, and H. R. Shea, "Large-stroke dielectric elastomer actuators with ion-implanted electrodes," *J. Microelectromech. Syst.* **18**(6), 1300–1308 (2009).

17. R. Pelrine, R. Kornbluh, Q. Pei, and J. Joseph, "High-speed electrically actuated elastomers with strain greater than 100%," *Science* **287**(5454), 836–839 (2000).

## 1. Introduction

Tunable optical lenses have given much attention for technical advances in optical communications, adaptive optical systems, and optical measurement systems [1, 2]. In particular, focus tunability for the optical lenses has been considered as a promising functionality for optical storage, microscopy, optical imaging devices with zoom in/out functions, and optical telescopes [3–6]. For a few decades, in order to realize tunable-focusing, many researchers have intensively studied liquid based tunable lenses, which are operating with fluidic actuations based pressure, electromagnetic wave, and electro-wetting [7–10]. Although the approaches have their own benefits, in adopting for commercial optical systems the liquid lenses still have technical challenges for securing scalability, gravity-insensitive property, consistent geometric shape, and thermal stability in wide temperature range.

As an alternative, tunable Fresnel lenses (TFLs) made with solid-state materials have been developed for focus-tunable optical systems due to their structural simplicity allowing miniaturized design. The TFLs mainly have been demonstrated by using liquid crystals (LCs) or mechanical stretching scheme [11, 12]. The LC based tunable lens is composed of a thin LC layer with binary Fresnel zone pattern and compliant electrodes with high optical transparency. The LC lens tunes its focal length by changing refractive index of the LC layer responding to control of voltage distribution across the electrodes. However, this lens has a technical difficulty in providing continuous focal length due to discrete change in period of Fresnel zone plate. The mechanical stretching based tunable lens made with optically transparent and elastomeric polydimethylsiloxane (PDMS) changes its focal length by radially stretching the lens with a mechanically controllable customized holder that consists of six symmetrically distributed clamps [12]. Although this methodology can allow continuous change in the focal length, the use of bulky mechanical components for stretching is not suitable for optical systems to require miniaturization and high speed operation.

In this paper, we propose a thin tunable binary phase Fresnel lens. The TFL is composed of a thin pre-stretched dielectric elastomer (DE) membrane with protrusive binary-phase microstructure at central area and annular complaint electrodes using silver nanowires (AgNWs). The TFL is capable of continuously modulating focal length responding to active-control of radius of Fresnel-zone using electrically-induced deformation behavior of DE actuator.

## 2. Tunable Fresnel lens based on a DE actuator

### 2.1 Design

Generally, a binary phase Fresnel lens is three-dimensional (3D) structure that consists of multiple transparent zones with periodic  $\pi$  phase shift as shown in Fig. 1(a). The radius of the  $N$ -th zone ( $R_N$ ) in a Fresnel lens is given by

$$R_N^2 = NR_1^2, \quad N = 1, 2, 3, \dots, \quad (1)$$

where  $R_1$  is the radius of the inner zone. Focal length ( $F$ ) of the lens is related to the zone number ( $N$ ), the zone radius ( $R_N$ ) and the wavelength of the incident light ( $\lambda$ ) [13],

$$F = \frac{R_1^2}{\lambda} = \frac{R_N^2}{N\lambda}, \quad (2)$$

When the radius of Fresnel lens decreases by the contracting factor ( $S$ ), the focal length can be decreased quadratically with respect to the factor,

$$F' = \frac{R_N'^2}{N\lambda} = \frac{(SR_N)^2}{N\lambda} = S^2 F, \quad (3)$$

where  $S = R_N' / R_N$ . It suggests that focal length of the Fresnel lens can be changed by controlling the radius of its zones as shown Fig. 1(b).

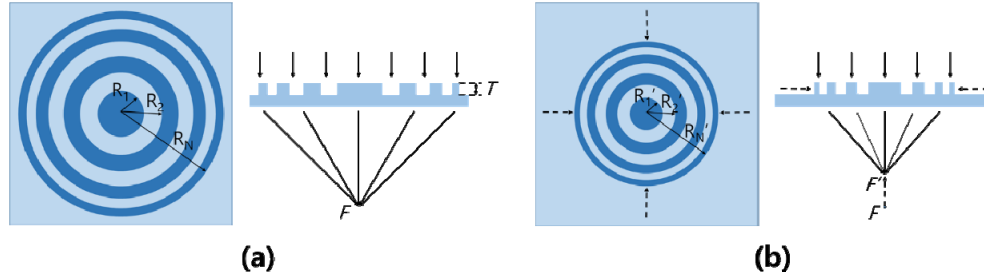


Fig. 1. Schematic diagram and operating principle of a tunable binary-phase Fresnel lens. Top view (left) and cross-section view (right) in (a) and (b). When the zones of the lens contract from (a) to (b), its focal length decreases from  $F$  to  $F'$ .

In order to realize all-solid-state TFL that can provide controllable focus in slim and lightweight configuration, we adopt electrically-induced deformation mechanism of DE membrane for physical contraction of the binary-phase microstructure. As illustrated in Fig. 2(a), the TFL is composed of a thin pre-stretched DE membrane with protrusive binary-phase microstructure at central area and annular compliant electrodes using AgNWs. In the binary-phase structure, the Fresnel zones are designed to be  $\pi$  phase shifted from each other on the incident light field as considering that the thickness of the lens ( $T$ ) satisfied by

$$T = \frac{\lambda}{2\Delta n}, \quad (4)$$

where  $\Delta n$  is the difference in refractive index ( $\Delta R_i$ ) between the neighboring zones. Notes that  $\Delta n$  for the proposed lens is  $\Delta R_i$  in between air and DE material. The TFL made with the DE material (optical refractive index: 1.41 at a wavelength of 0.6328 nm) has an initial focal length of 20 cm. When an electric potential applied across the pre-stretched DE membrane through annular electrodes, the DE membrane expands inwards responding to electro-static compression of the membrane under a blocked boundary condition. As the in-plane deformation induces mechanical contraction of central area, the radius of the zones becomes shorter as shown at Fig. 2(b).

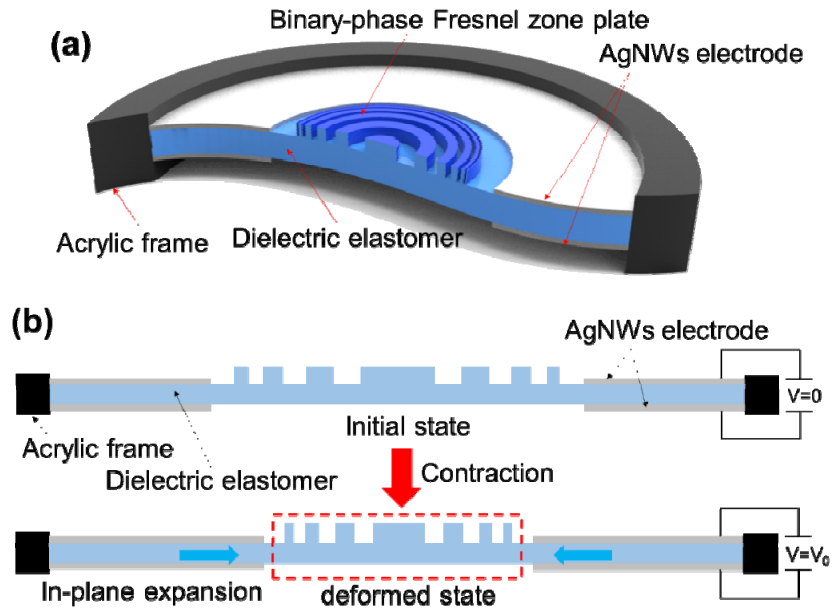


Fig. 2. (a) Structural configuration of the proposed TFL lens based on a DE membrane actuator. (b) Illustrated working principle for focus tuning of TFL: initial state ( $V = 0$ ) and deformed state responding to electrically-induced in-plane deformation of DE membrane ( $V = V_0$ ).

## 2.2 Fabrication

Figure 3 shows the schematic fabrication processes of the TFL. A photo-resist mold with intagliated microstructure for binary-phase Fresnel lens is fabricated on a silicon wafer by using a conventional photo-lithography process. A DE membrane with the protrusive microstructure is prepared by spin-casting a PDMS solution (a 1:1 mixture of a pre-polymer and a cross-linker of Elastosil P7670 supplied from Wacker Chemie AG) into the photo-resist mold, degassing in a vacuum chamber for 30 min at room temperature. After thermal cross-linking at 70°C for 1 hour, the DE structure is peeled off from the mold. The micro-structure formed on the DE membrane (thickness: 200  $\mu\text{m}$ , diameter: 50 mm) is designed to protrusive concentric rings with a consistent height of 3.2  $\mu\text{m}$ . In order to eliminate pull-in instability for stabilized large in-plane deformation [14], the DE structure is radially pre-stretched to 200% and the diameter of the micro-structure becomes 10 mm. And then it is fixed in between a couple of perforated acrylic frames. Finally, under a showdown mask, annular compliant electrode patterns are formed on both surfaces of the DE membrane by spay-coating AgNWs (average diameter:  $25 \pm 5$  nm and average length:  $35 \pm 5$   $\mu\text{m}$ ) dispersed in isopropyl alcohol and drying at room temperature. The nanowire electrode is highly conductive (sheet resistance ( $R_s$ ): as low as 10 $\Omega$ /sq) and mechanically robust against repetitive deformation of the DE membrane. Figure 3(h) shows a prototype of the TFL. Based on morphological observation using a 3D optical profiler, we assured that the Fresnel zone plate retains minimum zone-period of 4  $\mu\text{m}$  with a consistent height of about 0.8  $\mu\text{m}$  at its edge as shown in Fig. 3(i). It suggests that the structure satisfies the geometrical requirement for the binary-phase Fresnel lens as described in the Eq. (4).

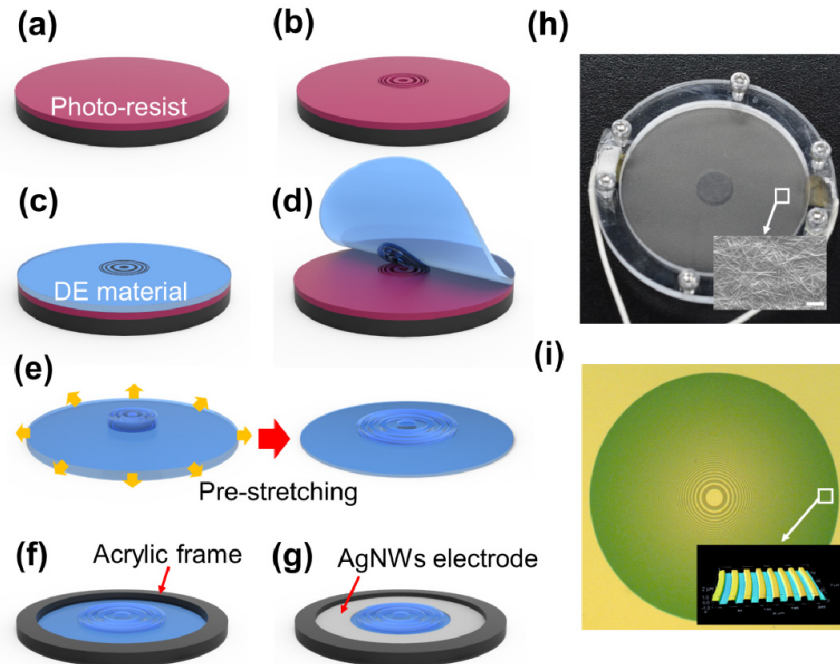


Fig. 3. An illustrated fabrication process of the TFL: (a) spin-casting photo-resist on a silicon wafer, (b) forming intagliated TFL structure, (c) spin-casting and thermal cross-linking of DE material, (d) peeling off the DE structure from the silicon wafer, (e) radially pre-stretching to 200%, (f) fixing with perforated acrylic frame, and (g) spray-coating the annular AgNWs electrode on both surfaces of the DE membrane under a shadow mask. A prototype of the TFL: (h) a photograph of the TFL and the AgNWs network for electrode (inset, scale bar: 2  $\mu\text{m}$ ), (i) microscopic images of the Fresnel zone structure and its magnified view at edge area (inset) observed using a PLu neox SensoFAR 3D optical profiler.

### 3. Characterization of the tunable Fresnel lens

#### 3.1 Change of focal length

Electrically-induced contraction of the Fresnel zones is evaluated by measuring change in diameter of the Fresnel zone plate during in-plane deformation of the DE membrane. Figure 4(a) shows electric voltage dependent contraction rate, which is defined as a percentage value for diameter change with respect to initial diameter of the Fresnel zone plate (diameter: 10 mm). The physical contraction results from inward expansion of the DE membrane under a blocked boundary condition [15, 16]. As an electric voltage operating the DE membrane increases to 4 kV, the contraction rate nonlinearly increases as high as 9.1%, presenting a profile similar to quadratic curve. The increasing trend follows a simple electro-static model presenting that the Maxwell pressure contracting the DE membrane in thickness direction can be increased in proportion to a square of electric field, explained by the equation below [17]:

$$p = \epsilon_0 \epsilon_r E^2 = \epsilon_0 \epsilon_r (V/t)^2, \quad (5)$$

where  $p$  is the effective pressure,  $\epsilon_0$  and  $\epsilon_r$  are the permittivity of free space and the relative permittivity (dielectric constant) of the polymer respectively;  $V$  is the applied voltage; and  $t$  is the thickness of the DE membrane. As shown in Fig. 4(a), there is a hysteresis effect between loading and unloading due to viscoelasticity of the lens material. The hysteresis is large at low driving voltage range and the phenomenon can be compensated by material improvement or

feedback control cooperating with an image sensor. This could be good future works to us for precise optical systems.

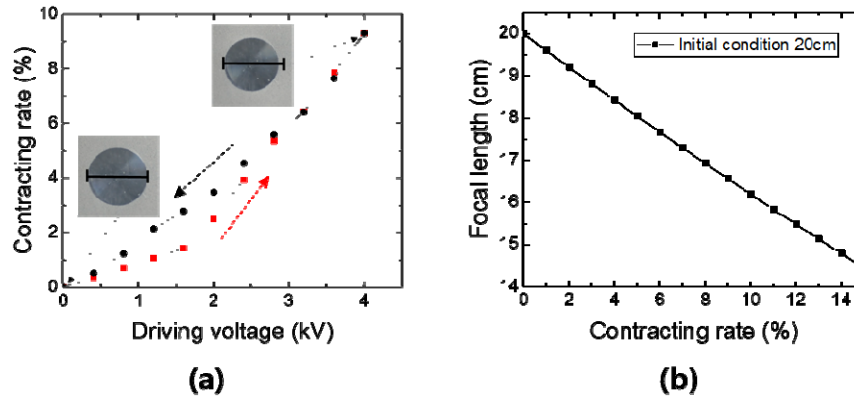


Fig. 4. (a) Electric voltage dependent contraction rate profile for the TFL, when driving the voltages upwards ( $\square$ ) and downwards ( $\circ$ ). The insets are photographs of the Fresnel zone plate before (0 V, lower left) and after contraction (4 kV, upper right). The bar scales in the insets are 10 mm. (b) Numerically calculated focal length with contracting rates.

In order to estimate influence of the contraction rate on change in focal length of the TFL, we numerically calculated the focal length with the contraction rate from the Eq. (3). As shown in Fig. 4(b), the focal length is inversely proportion to the contraction rate. Their correlation indicates that the initial focal length ( $F$ : 20 cm) can be tuned to 16.5 cm when the contraction rate becomes 9%.

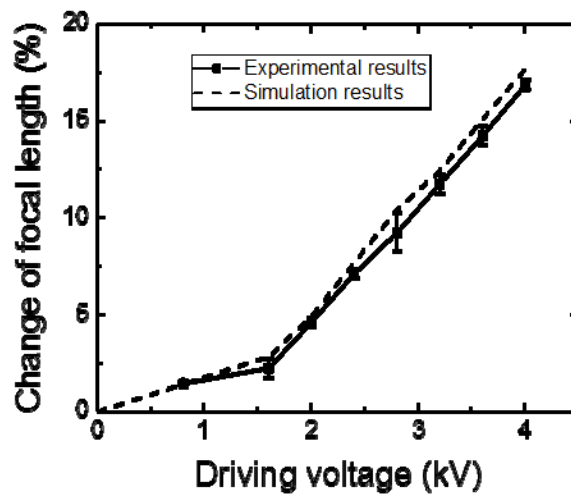


Fig. 5. Focal length change of the TFL under various driving voltages.

Based on the contraction response, change in focal length of the TFL with electric voltage is measured by using the optical setup which is composed of a He-Ne laser, two convex lens, a diaphragm, a translation-stage, and a camera. The focal length of the TFL is determined by observing a pattern of a focused light spot along optic axis. As shown in Fig. 5, the focal length decreases to 17.7% as the driving voltage increases to 4 kV. The trend is fairly consistent with numerical simulation performed under the same operating conditions using

the contraction rate, which is shown in Fig. 4(a). It indicates that the physical contraction resulting from the expansive deformation of the DE membrane is uniformly occurred at each zone in the Fresnel zone.

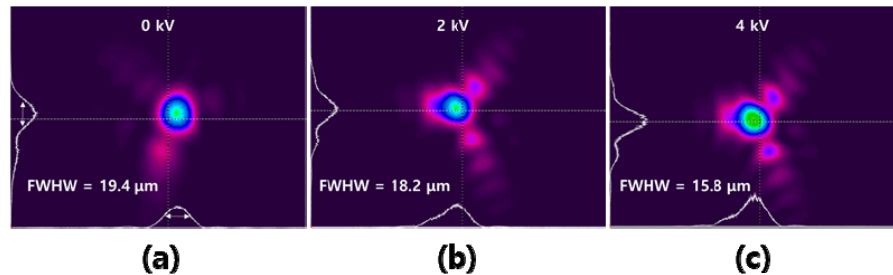


Fig. 6. Optical intensity distributions of the TFL on the focal planes under various driving voltages of (a) 0, (b) 2, and (c) 4 kV.

In order to investigate the optical quality of the TFL, optical intensity distributions and their FWHMs were measured at the focal planes for different applied voltages of 0, 2, and 4 kV as shown in Fig. 6. Based on the intensity pattern analysis, we found that the patterns present Gaussian distribution and the FWHMs decreased as the applied voltage increased. It indicates that the TFL possesses qualified geometry corresponding to a hemispherical convex lens. The artefacts around the focal spots appear due to asymmetry of the Fresnel structure and misalignment between the lens structure and electrode in the TFL. This can be improved as the manufacturing process matures.

### 3.2 Response property

Response time of the TFL is evaluated by measuring an optical intensity profile with time as powering on and off the TFL. For the test, an optical system is established as illustrated in Fig. 7(a). The test system enables a He-Ne laser beam passing through a spatial filter with a beam expander to be focused by the TFL and transmitted through an aperture (pin-hole) on the focal plane. During electrical operation of the TFL, a Si-detector monitors optical intensity of the beam at the focal spot. Figure 7(b) shows an optical intensity profile with time responding to an input voltage signal with square waveform. When the TFL is on-state by applying the voltage, the physical contraction of the Fresnel zone plate induces the beam focusing at the spot to be blurred. As becoming off-state, it rapidly recovers to initial condition. We calculated response time of the TFL as considering that the defocusing and focusing time of tunable lenses generally can be regarded as a time spent for 90% loss of an initial intensity and for 90% restoration from zero intensity, respectively. As the result, the TFL requires 23 ms for defocusing and 93 ms for focusing. Requirement of the focusing time, which is much longer than defocusing, is correlated to elasticity of the DE material for the TFL because the contracted TFL becomes the initial state only by restoration behavior of the material. Therefore, for shortening the focusing time, study for pre-stretching effect and improving elasticity of the DE material are remained as our future work.

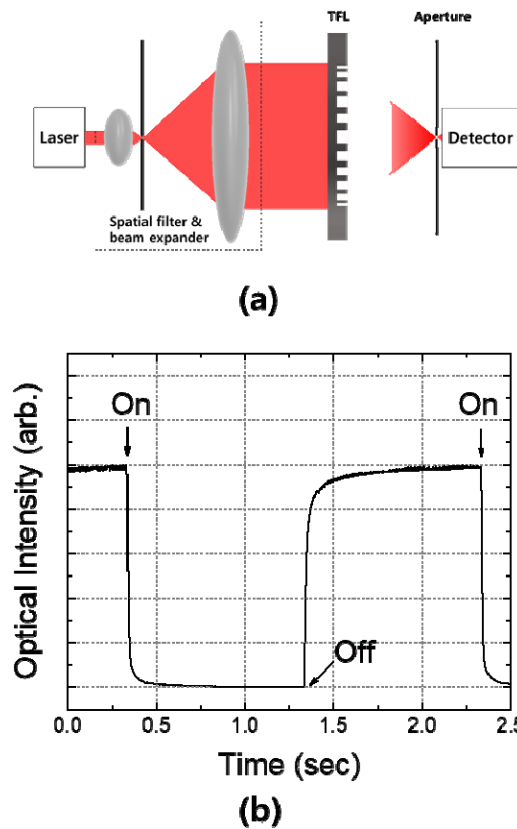


Fig. 7. (a) Experimental setup for characterizing the TFL. (b) Focusing (On state) and defocusing (Off state) response of the TFL as a function of time. Applied voltages to the lens are 2.4 kV for On and 0 kV for Off state.

#### 4. Summary

We have developed a thin tunable binary-phase Fresnel lens made with an electro-active DE material. The TFL changes its focal length responding to physical contraction of the Fresnel zone plate. The contraction is induced by in-plane deformation of the pre-stretched DE membrane that expands inwards under a blocked boundary condition. As expansive deformation increases with driving voltage, resultant increase in contraction shortens the radius of Fresnel-zone. Due to benefits from a functionality modulating geometry of the Fresnel zone plate with electric signal and structural simplicity allowing a thin film design, the TFL is capable of continuous changing focal length under a light-weight and compact configuration.

#### Funding

Pioneer Program of Korea National Research Foundation (2013M3C1A3059575); Creative Research Program of ETRI.

#### Acknowledgments

The authors would like to thank W. J. Shin for his support regarding fabrication process of materials.